Accepted Manuscript

Graphene oxide triggers mass transfer limitations on the methanogenic activity of an anaerobic consortium with a particulate substrate

J. Iván Bueno-López, J. Rene Rangel-Mendez, Felipe Alatriste-Mondragón, Fátima Pérez-Rodríguez, Virginia Hernández-Montoya, Francisco J. Cervantes

PII: S0045-6535(18)31469-3

DOI: 10.1016/j.chemosphere.2018.08.001

Reference: CHEM 21919

To appear in: *ECSN*

Received Date: 10 January 2018

Revised Date: 30 July 2018

Accepted Date: 1 August 2018

Please cite this article as: Bueno-López, J.Ivá., Rangel-Mendez, J.R., Alatriste-Mondragón, F., Pérez-Rodríguez, Fá., Hernández-Montoya, V., Cervantes, F.J., Graphene oxide triggers mass transfer limitations on the methanogenic activity of an anaerobic consortium with a particulate substrate, *Chemosphere* (2018), doi: 10.1016/j.chemosphere.2018.08.001.

Graphene oxide triggers mass transfer limitations on the methanogenic activity of an anaerobic consortium with a particulate substrate

J. Iván Bueno-López[a], J. Rene Rangel-Mendez[a,*], Felipe Alatriste-Mondragón[a], Fátima Pérez-Rodríguez[b], Virginia Hernández-Montoya[c] and Francisco J. Cervantes[a,*]

[a] División de Ciencias Ambientales, Instituto Potosino de Investigación Científica y Tecnológica (IPICyT), Camino a la Presa San José 2055, Col. Lomas 4a. Sección, 78216 San Luis Potosí, SLP, Mexico

[b] CONACYT- Instituto Potosino de Investigación Científica y Tecnológica (IPICyT), Camino a la Presa San José 2055, Col. Lomas 4a. Sección, 78216 San Luis Potosí, SLP, Mexico

[c] Instituto Tecnológico de Aguascalientes, Av. Adolfo López Mateos No. 1801 Ote., 20256, Aguascalientes, Ags., Mexico

[*] Corresponding authors. Tel.: +52 444 834 2041; fax: +52 444 834 2010.

E-mail address: rene@ipicyt.edu.mx (J.R. Rangel-Mendez) and fjcervantes@ipicyt.edu.mx (F.J. Cervantes)

Abstract

Graphene oxide (GO) is an emerging nanomaterial widely used in many manufacturing applications, which is frequently discharged in many industrial effluents eventually reaching biological wastewater treatment systems (WWTS). Anaerobic WWTS are promising technologies for renewable energy production through biogas generation; however, the effects of GO on anaerobic digestion are poorly understood. Thus, it is of paramount relevance to generate more knowledge on these issues to prevent that anaerobic WWTS lose their effectiveness for the removal of pollutants and for biogas production. The aim of this work was to assess the effects of GO on the methanogenic activity of an anaerobic consortium using a particulate biopolymer (starch) and a readily fermentable soluble substrate (glucose) as electron donors. The obtained results revealed that the methanogenic activity of the anaerobic consortium supplemented with starch decreased up to 23-fold in the presence of GO compared to the control incubated in the absence of GO. In contrast, we observed a modest improvement on methane production (>10% compared to the control lacking GO) using 5 mg of GO L^{-1} in glucose-amended incubations. The decrease in the methanogenic activity is mainly explained by wrapping of starch granules by GO, which caused mass transfer limitation during the incubation. It is suggested that wrapping is driven by electrostatic interactions between negatively charged oxygenated groups in GO and positively charged hydroxyl groups in starch. These results imply that GO could seriously hamper the removal of particulate organic matter, such as starch, as well as methane production in anaerobic WWTS.

Keywords: graphene oxide; starch; anaerobic digestion; mass transfer limitation

1. Introduction

Nanotechnology is growing at vertiginous speed and everyday more goods containing nanomaterials are available in the market, from food to hi-tech applications (Vance et al., 2015). Unfortunately, the eventual negative effects of tailored nanoparticles on human health and on ecosystems are unknown. Moreover, there are some important knowledge gaps with regard to analytical methods for nanoparticles detection and also lack of legislation to establish guidelines and regulations to ensure the proper and safety management and disposal of nanomaterials-containing residues (Eduok et al., 2013). This is the outcome of poor understanding of the interactions between different nanomaterials and cellular constituents, both in engineered systems and in natural environments (He et al., 2014; Hu et al., 2016; Trujillo-Reyes et al., 2014).

Graphene and graphene oxide (GO) are two of the nanomaterials that have gained a lot of attention due to their interesting properties. GO is used as an intermediate to obtain graphene after its reduction (or reduced GO, rGO for short, since in most cases some oxygenated groups remain on graphitic sheets) (Bagri et al., 2010; Mattevi et al., 2009). Besides, GO contains a range of oxygenated functional groups that can be exploited as anchoring sites for functionalization and its production is inexpensive and easily scalable (Dreyer et al., 2010; Novoselov et al., 2012; Zhao et al., 2014); this is the reason why it is used in many processes and products.

Due to their widespread application, graphene and GO are frequently discharged in several industrial wastewaters, which ultimately reach biological WWTS. Anaerobic digestion is increasingly considered as the best option for wastewater treatment, but given the scenario in which nanomaterials are common components in industrial processes, the arrival of nanomaterials to WWTS is expected, where they will interact with organic matter and cells, eventually affecting the anaerobic digestion process (Yang et al., 2015; Zhao et al., 2014).

Starch is one of the most abundant biopolymers in the world and has been largely used in food industry for human and animal nutrition. Moreover, it is also employed in other applications, such

as laundry services and the production of paper, pharmaceuticals, textiles, and biodegradable products. This scenario has given rise to industries generating effluents with high levels of chemical oxygen demand (COD) due to the presence of residual starch (Lu et al., 2015; Şentürk et al., 2010; Vanier et al., 2017).

GO and its derivatives have also been intensively used in process treatments to remove pathogens, as well as organic and inorganic compounds from gaseous, aqueous and solid media (Shen et al., 2018; Trujillo-Reyes et al., 2014; Wang et al., 2013). They have also been explored as redox mediators in anaerobic systems to enhance the biotransformation of recalcitrant compounds (Colunga et al., 2015; Toral-Sánchez et al., 2017; Wang et al., 2014). Additionally, other studies report on the implementation of graphene as a conductive component in biological systems that facilitates direct interspecies electron transfer (DIET), resulting in enhanced methane production (Lin et al., 2017; Lü et al., 2018; Tian et al., 2017); and functionalized GO has even been used as growth stimulator for engineered bacteria (Luo et al., 2016). Therefore, it is conceivable that GO and starch coexist in several industrial discharges.

Nevertheless, recent literature related to the effects of GO on methanogenic activity by anaerobic consortia shows contradictory results and there are no data referring to the effect of combined systems, such as GO-starch, and their effects on anaerobic digestion, to the best of our knowledge. Hence, the objective of this work was to assess the effects of GO on the methanogenic activity of an anaerobic consortium, which was fed with a complex polymer (starch) or with a soluble readily fermentable substrate (glucose). This information contributes to elucidate the effects of GO on anaerobic WWTS, which ultimately has relevance to achieve effective anaerobic treatment of industrial effluents to produce bioenergy.

2. Materials and methods

2.1. Materials and chemical reagents

GO was purchased from Graphene Supermarket®, which has the following characteristics: concentration 6.2 g L^{-1} in aqueous dispersion, monolayer > 80%, nominal particle size between 0.5 and 5 µm, C/O ratio 3.95. Starch, glucose and all the reagents used in this work were reactive grade from Sigma-Aldrich Company.

2.2. Solutions

The basal medium used during sludge activation was composed of (mg L^{-1}): NH_4Cl (280), K_2HPO_4 (250), $MgSO_4 \cdot 7H_2O$ (100), $CaCl_2 \cdot 2H_2O$ (10), $NaHCO_3$ (5000) and 1 mL of trace elements solution composed of (mg L^{-1}): $FeCl_2 \cdot 4H_2O$ (2000), H_3BO_3 (50), $ZnCl_2$ (50), $CuCl_2 \cdot 2H_2O$ (38), $MnCl_2 \cdot 4H_2O$ (500), $(NH_4)_6Mo_7O_{24} \cdot 4H_2O$ (50), $AlCl_3 \cdot 6H_2O$ (90), $CoCl_2 \cdot 6H_2O$ (2000), $NiCl_2 \cdot 6H_2O$ (92), $Na_2SeO_3 \cdot 6H_2O$ (162), EDTA (1000) and 1 mL HCl (36%); pH was adjusted to 7.0 ± 0.2 using NaOH or HCl 0.1 N if needed. In the case of batch assays, $NaHCO_3$ (3.13 g L^{-1}) was used to get a pH of 7 in combination with a mixture of N_2/CO_2 (80/20 v/v) used as headspace. Distilled water was used to prepare all solutions.

Using the basal medium described above, a starch stock of 100 mg COD L^{-1} was prepared by adding the proper amount of starch powder and mixing with magnetic stirring for 30 min. Using volumetric flasks of 100 mL, GO dispersions of 5, 25, 50, 152.5 and 300 mg L^{-1} were prepared, taking aliquots from the concentrated GO dispersion, adding to the volumetric flask and filling up to the 100 mL mark with the starch stock prepared before. The resulting mix was sonicated for 30 min prior to be placed into the incubation bottles.

2.3. Inoculum

Anaerobic sludge from a full-scale up-flow anaerobic sludge blanket (UASB) reactor treating effluents from a candy factory (San Luis Potosí, Mexico) was used as inoculum in the batch experiments. The sludge was acclimated for three months in a lab-scale UASB reactor (1.5 L) under methanogenic conditions at a hydraulic residence time (HRT) of 1 day, with 1 g COD L^{-1} of glucose as energy source at 25°C. The efficiency of the reactor, in terms of COD removal, was up to 90%

under steady state conditions. Volatile suspended solids (VSS) content was 3.22% respect to wet weight.

2.4. Characterization of materials.

2.4.1. Spectroscopic characterization

Identification of surface functional groups of materials was carried out using KBr pellets, prepared with a 99%/1% (w/w) KBr/material proportion, which were analyzed at 32 scans with a 4 cm^{-1} resolution in a Thermo-Scientific Fourier Transform Infrared (FT-IR) spectrophotometer (Nicolet 6700) under ambient conditions. GO material was obtained by drying 500 µL of the concentrated dispersion, while GO-starch mixture was prepared using 2:1 (GO:Starch) ratio by mixing 322.6 µL of the concentrated GO dispersion and 1 mg of starch and then sonicated for 20 min. Both GO and GO-starch mixture were dried for 4 h at 45°C and 1400 rpm under vacuum (Vacufuge plus Eppendorf). Raman spectra were recorded with RENISHAW Micro-Raman spectrometer with a laser frequency of 633 nm at a potency of 10% through a 50× objective. Elemental composition, oxidation states of the elements and information about the structure of GO surface were obtained through X-ray photoelectron spectroscopy (XPS) analysis. Sample preparation consisted of a GO dripping deposition on a silicon wafer, dried at room temperature for 12 h and the resulting film was analyzed using a PHI 5000 VersaProbe II equipment with a monochromatic X-ray beam source at 1486.6 eV and 15 kV. The obtained spectra were deconvoluted with help of Aanalyzer software v1.27, and the elemental composition was acquired with CasaXPS software v2.3.18PR1.0.

2.4.2. Particle charge and size distribution

Size distribution and zeta potential (ζ) of GO and starch were obtained using a MICROTRAC Zetatrac NPA152-31A equipment. Each sample was sonicated for 10 s before zeta potential measurement. For size distribution, starch was suspended in deionized water at 500 mg L^{-1} and

mixed for 30 min before measurement, while a dispersion of 150 mg L^{-1} in deionized water was used for GO.

Zeta potential was obtained using deionized water and basal medium as dispersants, considering a pH range from 6 to 8 obtained by adding NaOH or HCl 0.1 N as needed. Mixtures of GO (5 mg L^{-1}) and starch (150 mg L^{-1}) in deionized water and basal medium were prepared following the same procedure described above for starch, and then GO was added. The resulting mixture was sonicated for 10 min before being placed into polypropylene tubes to adjust pH to the desired values.

Dissociation constants (pKa) of GO functional groups were determined by potentiometric titration (METTLER TOLEDO T70), employing mixtures of 5 mg of GO in 20 mL of NaCl 0.01 N solution. The mixtures obtained were left for 12 h at room temperature under mixing at 130 rpm. After this time, pH was adjusted to 3 by adding HCl 0.1 N and then titrated using NaOH 0.1 N until the solution reached a pH value of 12. The resulting titration data were analyzed using SAEIU-pK-Dist© software to get the pKa distribution (Jagiello et al., 1995).

2.4.3. Scanning electron microscopy (SEM)

Micrographs of GO, starch, sludge and their mixtures were obtained with a FEI Helios Nanolab 600 Dual Beam Scanning Electron Microscope, operated at 5.00 kV and 86 pA. Samples were mounted on aluminum pins by dripping deposition. In the case of GO and the sludge, deionized water and basal medium were used as dispersant, respectively, while two different samples were prepared for starch: (1) powder was placed on carbon tape; and (2) a few drops of starch dispersed in deionized water. All samples were dried at atmospheric conditions overnight before being observed and studied under the microscope.

2.5. Methanogenic activity tests

Methane production was evaluated in batch experiments by duplicate, using 120-mL glass serum bottles in which 600 mg VSS L^{-1} were inoculated into 50 mL GO-starch dispersion. In these experiments, starch was the substrate for microbial growth, while to assess the impact of the type of

substrate and study the influence of possible GO-starch interactions, a set of experiments were carried out using glucose as substrate. Both substrates were supplied at a concentration of 100 mg COD L^{-1}. Glucose was added just before incubation to prevent GO reduction (Ma et al., 2013). Control experiments without GO were performed to define the effect of GO itself on methanogenesis. Anaerobic conditions were kept along the inoculation process under N_2/CO_2 (80/20 v/v) atmosphere and incubation was performed in the dark at 25°C. Cumulative methane production was measured by gas chromatography using an Agilent equipment model 6890N, under previously reported conditions (Valenzuela et al., 2017), sampling gas phase every 5 h in the case of glucose and every 10 h for starch. Liquid samples were taken every 10 h to measure volatile fatty acids (VFAs) by capillary electrophoresis (Agilent 1600A equipment), as described elsewhere (Arriaga et al., 2011). All samples were previously centrifuged and filtered through 0.22 µm nitrocellulose membranes.

3. Results and discussion

3.1. Effects of GO on methanogenic sludge

In order to elucidate the limiting steps affected by GO on anaerobic digestion, two different substrates were considered in the assessments: a soluble readily fermentable substrate (glucose) and a particulate complex polymer (starch) that depends on its hydrolysis to be converted during methanogenesis. Methane quantification (Fig. 1) revealed that conversion of starch into methane occurred at a lower rate as compared to that observed with glucose (6.8 and 10 mmol h^{-1}, respectively). In addition, the results of methane production also indicated a negative effect with the increase in GO concentration in both cases. In fact, incubations performed with starch were more affected by GO on the methanogenic activity compared to incubations supplied with glucose as electron donor.

Interestingly, the lowest tested concentration of GO (5 mg L^{-1}) showed a positive effect on methane

187 production (>10% increase compared to the control incubated without GO) when glucose was
188 supplied as an electron donor. This improvement could be due to the conductivity of the rGO sheets
189 that promote DIET by syntrophic associations between bacteria and methanogens or due to GO
190 redox-mediating capacity (Colunga et al., 2015; Feng et al., 2013; Ma et al., 2013; Salas et al.,
191 2010; Salvador et al., 2017; Wang et al., 2011; Xu et al., 2015).
192 SEM images show that starch granules in powder form have smooth appearance (Fig. 2a), while
193 those dispersed in water have rugged surface (Fig. 2b), which indicates that starch granules partially
194 dissolve in the medium. In Fig. 2c and 2d, it is clearly visible a homogeneous coverage of starch
195 granules by GO sheets. Most GO sheets have a size around 687 nm, while prevalent size of starch is
196 around 102.2 nm (Fig. 3). This last value agrees with the size of the hierarchical structures that form
197 starch granules (Fig. S1a, Supplementary data (SD)), called blocklet (Fig. S1a inset in SD) (Pérez
198 and Bertoft, 2010), suggesting that, in the absence of GO, starch granules in suspension are
199 separated into blocklets during sonication. While starch granules might have had larger size when
200 dispersed in the basal medium used in sludge incubations, they were clearly covered by multiple
201 GO sheets (Fig. 2). The wrapping of starch granules by GO observed here could prevent starch
202 hydrolysis and limit substrate available to cells, consequently leaving only the soluble starch
203 fraction for methanogenesis, explaining the low methane values observed when starch was
204 employed as electron donor.
205 Besides methane measurements, VFAs were also quantified during the incubations (data not
206 shown); nevertheless, results showed concentrations under the detection limit for all VFAs
207 monitored, including acetate, propionate, lactate and butyrate, in all samples taken throughout the
208 incubation period. These results imply that VFAs were readily used as soon as they were produced
209 either from glucose fermentation or from starch hydrolysis, which suggests that methanogenesis
210 was probably not inhibited by GO during the incubation.
211 Mass transfer limitation imposed by GO coating on starch granules might have not been the only
212 mechanism responsible for the low of methane production observed, since it is also expected a

213 wrapping of cells because peptidoglycan, pseudo-peptidoglycan (for archaea (Bullock, 2000)) and
214 other cell components have functional groups that could interact via hydrogen bonding, π-π
215 interactions and electrostatic adsorption with GO (Zou et al., 2016). These interactions might have
216 decreased methane production in experiments amended with glucose, which was completely
217 solubilized and thus the sequestering effect of substrate can be discarded. These suggestions are
218 supported by reports, which demonstrated cells coverage by GO and correlated its inactivation
219 capacity to its lateral dimension, that is, bigger GO sheets are more effective inactivating cells in a
220 short time due to cell isolation (Liu et al., 2012) while small particles can enter the cytoplasm,
221 especially those with positive charge, causing oxidative stress (Hu et al., 2017; Hu and Zhou, 2013).
222 In addition, the presence of cations in the basal medium has to be considered; it has been reported
223 that GO, in the presence of organic matter or bacteria and low concentrations of divalent cations,
224 forms flocs due to bridging effect between cations and GO functional groups (Chowdhury et al.,
225 2015; Zhang et al., 2013).
226 Wrapping of cells by rGO could also be plausible, considering that GO can be reduced by glucose
227 (Ma et al., 2013), starch (Feng et al., 2013) and bacteria (De Silva et al., 2017; Salas et al., 2010),
228 causing aggregation of graphene and trapping bacteria within the aggregated sheets in the process
229 (Akhavan et al., 2011). SEM images show cells and sludge flocs covered by GO (Fig. S2 in SD);
230 however, further studies are needed to clarify the interactions between GO and anaerobic
231 microorganisms present in methanogenic consortia.

232 **3.2. Interactions between GO and starch affecting anaerobic digestion**

233 According to ζ results obtained with deionized water, the expected interaction is electrostatic
234 attraction due to positive charges of starch and negative ones on GO in the pH range of interest. It is
235 possible to find a change of charge when the mixture GO-starch goes from pH = 6 to pH = 7, from
236 24.5 mV to 2.46 mV, respectively (SD, Fig. S3). This drop in charge agrees with the pK_a of ~6.6
237 found in GO characterization (SD, Fig. S4), corresponding to deprotonation of carboxylic groups

and it results in charge neutralization with the positive charge of hydroxyl groups of starch that stay with positive charge at those pH values. Even though C1s XPS results (Fig. 4) indicate that carboxylic groups (at 289.3 eV) are just a fraction of the total GO functional groups, they could be the main responsible for built up negative charges (Konkena and Vasudevan, 2012), favoring the attraction of starch and then triggering the interaction with other GO groups. Other groups found through C1s XPS are C=C (284.5 eV) and their associated π-π^* shake-up of the aromatic system (291.4 eV), as well as C=O (288.3 eV) and C-O (287.4) (Castro et al., 2016), which have higher intensities than carboxylic groups.

In O1s XPS spectrum (Fig. 5), the peak with the largest area at ~533.1 eV can be assigned to the combined effects of singly bonded oxygen, followed in decreasing order, by a peak at 532.5 eV assigned to C=O in carbonyl and/or carboxyl groups and finally by the peak at 533.8 eV corresponding to hydroxyl groups (mainly in phenolic compounds) (Hantsche, 1993; Levi et al., 2015; Puziy et al., 2008). In both C1s and O1s XPS spectra, single bonds between carbon and oxygen are predominant. In addition, the concentration of oxygen-containing groups (phenolic, carbonyl and carboxylic) obtained by Boehm titration (SD, Table S1), agrees with that reported by XPS analysis.

Interaction between GO and starch functional groups were studied by FT-IR (Fig. 6), finding out a shift in peaks at 1730 cm^{-1}, 1570 cm^{-1}, 1200 cm^{-1}, 1100 cm^{-1} and 600 cm^{-1} to 1646 cm^{-1}, 1414 cm^{-1}, 1169 cm^{-1}, 998 cm^{-1} and 570 cm^{-1}; related with C=O, C=C, C-O-C (epoxide), C-O and phenolic groups, respectively. These shifts have been attributed to hydrogen bonding, in the case of the oxygenated groups (Li et al., 2011; Socrates, 2004; Xu et al., 2016), and to Lewis acid-base interaction for C=C in aromatic rings (Zhao et al., 2014). These results and those from ζ data suggest that the wrapping observed by SEM images is due to interactions that possibly include hydrogen bonding, which implies that the GO coating is tightly bound and as a result interferes with the hydrolysis of the starch, as indicated in the previous section.

FT-IR of GO-starch mixtures show a narrowing and improvement in definition of band at ~3300 cm^{-1} assigned to –OH. This band is broader in the spectrum of GO alone (Fig. 6); A broader band shape has been associated with the presence of water either intercalated among stacks of GO or physisorbed on GO sheets (Acik et al., 2011), so the narrower band of GO-starch mixtures suggests a decrease in water amount due to a conformation of stacks with fewer layers on the surface of starch granules. The relevance of the above lies on the possible development of "blade like edge" that can damage cell membrane (Cai et al., 2011); however, no evidence of this phenomenon was found; even when GO appears to have single or few sheets in the incubations with glucose (SD, Fig S1b) or starch. It is important to note that stacks of some sheets were seen when GO was dried without being in contact with starch or sludge (Fig. S1b inset in SD).

3.3. Environmental relevance

The results presented in this study showed that starch granules can be wrapped by GO sheets preventing their hydrolysis, which is the initial step for their conversion to methane under anaerobic conditions, leading to poor methane production. This scenario represents a challenge to anaerobic wastewater treatment systems, as removal of pollutants from industrial effluents to produce renewable energy (as biogas) can be seriously hampered, especially in the case of effluents of food and other industrial sectors containing starch as the main COD fraction.

In natural ecosystems, the wrapping of particulate organic matter (POM) by GO could affect the availability of nutrients for heterotrophic organisms, thus altering the trophic web or cause a disruption of the dynamic interchange between POM and dissolved organic matter (DOM), that may result in major disequilibrium of ecosystems since both DOM and POM are involved in complex biogeochemical cycles.

4. Conclusions

This study elucidates, for the first time, mass transfer limitation imposed by GO on the methanogenic activity by an anaerobic consortium. Collected evidence indicated that wrapping of starch granules was the main mechanism involved. The results also reveal that low concentration of GO may enhance the methanogenic activity of the anaerobic consortium studied, presumably driven by DIET, during glucose fermentation. This information contributes to shed light on the effects of GO on anaerobic WWTS.

Acknowledgements

The program Frontiers in Science of CONACYT (Project 1289) financially supported this work. J.I. Bueno-López thanks for the scholarship received from Tecnológico Nacional de México (TecNM). Additionally, authors acknowledge the technical support provided by D. Partida-Gutiérrez, G. Vidriales-Escobar, J.P. Rodas-Ortiz, M. Delgado-Cardoso and E. Vences-Alvarez. We also greatly acknowledge M. Bravo-Sánchez, A.I. Peña-Maldonado and B. Rivera-Escoto for XPS, SEM and Raman analysis, respectively, at Nanoscience and Nanotechnology Research National Laboratory (LINAN-IPICyT).

References

Acik, M., Lee, G., Mattevi, C., Pirkle, A., Wallace, R.M., Chhowalla, M., Cho, K., Chabal, Y., 2011. The Role of Oxygen during Thermal Reduction of Graphene Oxide Studied by Infrared Absorption Spectroscopy. J. Phys. Chem. C 115, 19761–19781. https://doi.org/10.1021/jp2052618

Akhavan, O., Ghaderi, E., Esfandiar, A., 2011. Wrapping Bacteria by Graphene Nanosheets for Isolation from Environment, Reactivation by Sonication, and Inactivation by Near-Infrared Irradiation. J. Phys. Chem. B 115, 6279–6288. https://doi.org/10.1021/jp200686k

Arriaga, S., Rosas, I., Alatriste-Mondragón, F., Razo-Flores, E., 2011. Continuous production of

hydrogen from oat straw hydrolysate in a biotrickling filter. Int. J. Hydrogen Energy 36, 3442–3449. https://doi.org/10.1016/j.ijhydene.2010.12.019

Bagri, A., Mattevi, C., Acik, M., Chabal, Y.J., Chhowalla, M., Shenoy, V.B., 2010. Structural evolution during the reduction of chemically derived graphene oxide. Nat. Chem. 2, 581–587. https://doi.org/10.1038/nchem.686

Bullock, C., 2000. The Archaea-a biochemical perspective. Biochem. Mol. Biol. Educ. 28, 186–191. https://doi.org/10.1111/j.1539-3429.2000.tb00142.x

Cai, X., Tan, S., Lin, M., Xie, A., Mai, W., Zhang, X., Lin, Z., Wu, T., Liu, Y., 2011. Synergistic Antibacterial Brilliant Blue/Reduced Graphene Oxide/Quaternary Phosphonium Salt Composite with Excellent Water Solubility and Specific Targeting Capability. Langmuir 27, 7828–7835. https://doi.org/10.1021/la201499s

Castro, K.L.S., Curti, R. V., Araujo, J.R., Landi, S.M., Ferreira, E.H.M., Neves, R.S., Kuznetsov, A., Sena, L.A., Archanjo, B.S., Achete, C.A., 2016. Calcium incorporation in graphene oxide particles: A morphological, chemical, electrical, and thermal study. Thin Solid Films 610, 10–18. https://doi.org/10.1016/j.tsf.2016.04.042

Chowdhury, I., Mansukhani, N.D., Guiney, L.M., Hersam, M.C., Bouchard, D., 2015. Aggregation and Stability of Reduced Graphene Oxide: Complex Roles of Divalent Cations, pH, and Natural Organic Matter. Environ. Sci. Technol. 49, 10886–10893. https://doi.org/10.1021/acs.est.5b01866

Colunga, A., Rangel-Mendez, J.R., Celis, L.B., Cervantes, F.J., 2015. Graphene oxide as electron shuttle for increased redox conversion of contaminants under methanogenic and sulfate-reducing conditions. Bioresour. Technol. 175, 309–314. https://doi.org/10.1016/j.biortech.2014.10.101

De Silva, K.K.H., Huang, H.-H., Joshi, R.K., Yoshimura, M., 2017. Chemical reduction of graphene oxide using green reductants. Carbon N. Y. 119, 190–199. https://doi.org/10.1016/j.carbon.2017.04.025

339 Dreyer, D.R., Park, S., Bielawski, C.W., Ruoff, R.S., 2010. The chemistry of graphene oxide.
340 Chem. Soc. Rev. 39, 228–240. https://doi.org/10.1039/b917103g
341 Eduok, S., Martin, B., Villa, R., Nocker, A., Jefferson, B., Coulon, F., 2013. Evaluation of
342 engineered nanoparticle toxic effect on wastewater microorganisms: Current status and
343 challenges. Ecotoxicol. Environ. Saf. 95, 1–9. https://doi.org/10.1016/j.ecoenv.2013.05.022
344 Feng, Y., Feng, N., Du, G., 2013. A green reduction of graphene oxide via starch-based materials.
345 RSC Adv. 3, 2146621474. https://doi.org/10.1039/c3ra43025a
346 Hantsche, H., 1993. High resolution XPS of organic polymers, the scienta ESCA300 database. Adv.
347 Mater. 5, 778–778. https://doi.org/10.1002/adma.19930051035
348 He, X., Aker, W.G., Leszczynski, J., Hwang, H.M., 2014. Using a holistic approach to assess the
349 impact of engineered nanomaterials inducing toxicity in aquatic systems. J. Food Drug Anal.
350 22, 128–146. https://doi.org/10.1016/j.jfda.2014.01.011
351 Hu, L., Wan, J., Zeng, G., Chen, A., Chen, G., Huang, Z., He, K., Cheng, M., Zhou, C., Xiong, W.,
352 Lai, C., Xu, P., 2017. Comprehensive evaluation of the cytotoxicity of CdSe/ZnS quantum
353 dots in Phanerochaete chrysosporium by cellular uptake and oxidative stress. Environ. Sci.
354 Nano 4, 2018–2029. https://doi.org/10.1039/C7EN00517B
355 Hu, X., Li, D., Gao, Y., Mu, L., Zhou, Q., 2016. Knowledge gaps between nanotoxicological
356 research and nanomaterial safety. Environ. Int. 94, 8–23.
357 https://doi.org/10.1016/j.envint.2016.05.001
358 Hu, X., Zhou, Q., 2013. Health and ecosystem risks of graphene. Chem. Rev. 113, 3815–3835.
359 https://doi.org/10.1021/cr300045n
360 Jagiello, J., Bandosz, T.J., Putyera, K., Schwarz, J.A., 1995. Determination of Proton Affinity
361 Distributions for Chemical Systems in Aqueous Environments Using a Stable Numerical
362 Solution of the Adsorption Integral Equation. J. Colloid Interface Sci. 172, 341–346.
363 https://doi.org/10.1006/jcis.1995.1262
364 Konkena, B., Vasudevan, S., 2012. Understanding aqueous dispersibility of graphene oxide and

reduced graphene oxide through pKa measurements. J. Phys. Chem. Lett. 3, 867–872. https://doi.org/10.1021/jz300236w

Levi, G., Senneca, O., Causà, M., Salatino, P., Lacovig, P., Lizzit, S., 2015. Probing the chemical nature of surface oxides during coal char oxidation by high-resolution XPS. Carbon N. Y. 90, 181–196. https://doi.org/10.1016/j.carbon.2015.04.003

Li, R., Liu, C., Ma, J., 2011. Studies on the properties of graphene oxide-reinforced starch biocomposites. Carbohydr. Polym. 84, 631–637. https://doi.org/10.1016/j.carbpol.2010.12.041

Lin, R., Cheng, J., Zhang, J., Zhou, J., Cen, K., Murphy, J.D., 2017. Boosting biomethane yield and production rate with graphene: The potential of direct interspecies electron transfer in anaerobic digestion. Bioresour. Technol. 239, 345–352. https://doi.org/10.1016/j.biortech.2017.05.017

Liu, S., Hu, M., Zeng, T.H., Wu, R., Jiang, R., Wei, J., Wang, L., Kong, J., Chen, Y., 2012. Lateral Dimension Dependent Antibacterial Activity of Graphene Oxide Sheets. Langmuir. https://doi.org/10.1021/la3023908

Lü, F., Guo, K.J., Duan, H.W., Shao, L.M., He, P.J., 2018. Exploit Carbon Materials to Accelerate Initiation and Enhance Process Stability of CO Anaerobic Open-Culture Fermentation. ACS Sustain. Chem. Eng. 6, 2787–2796. https://doi.org/10.1021/acssuschemeng.7b04589

Lu, X., Zhen, G., Estrada, A.L., Chen, M., Ni, J., Hojo, T., Kubota, K., Li, Y.-Y., 2015. Operation performance and granule characterization of upflow anaerobic sludge blanket (UASB) reactor treating wastewater with starch as the sole carbon source. Bioresour. Technol. 180, 264–273. https://doi.org/10.1016/j.biortech.2015.01.010

Luo, Y., Yang, X., Tan, X., Xu, L., Liu, Z., Xiao, J., Peng, R., 2016. Functionalized graphene oxide in microbial engineering: An effective stimulator for bacterial growth. Carbon N. Y. 103, 172–180. https://doi.org/10.1016/j.carbon.2016.03.012

Ma, T., Chang, P.R., Zheng, P., Ma, X., 2013. The composites based on plasticized starch and graphene oxide/reduced graphene oxide. Carbohydr. Polym. 94, 63–70.

https://doi.org/10.1016/j.carbpol.2013.01.007

Mattevi, C., Eda, G., Agnoli, S., Miller, S., Mkhoyan, K.A., Celik, O., Mastrogiovanni, D., Granozzi, G., Carfunkel, E., Chhowalla, M., 2009. Evolution of electrical, chemical, and structural properties of transparent and conducting chemically derived graphene thin films. Adv. Funct. Mater. 19, 2577–2583. https://doi.org/10.1002/adfm.200900166

Novoselov, K.S., Fal'ko, V.I., Colombo, L., Gellert, P.R., Schwab, M.G., Kim, K., 2012. A roadmap for graphene. Nature 490, 192–200. https://doi.org/10.1038/nature11458

Pérez, S., Bertoft, E., 2010. The molecular structures of starch components and their contribution to the architecture of starch granules: A comprehensive review. Starch/Staerke. https://doi.org/10.1002/star.201000013

Puziy, A.M., Poddubnaya, O.I., Socha, R.P., Gurgul, J., Wisniewski, M., 2008. XPS and NMR studies of phosphoric acid activated carbons. Carbon N. Y. 46, 2113–2123. https://doi.org/10.1016/j.carbon.2008.09.010

Salas, E.C., Sun, Z., Lüttge, A., Tour, J.M., 2010. Reduction of Graphene Oxide via Bacterial Respiration. ACS Nano 4, 4852–4856. https://doi.org/10.1021/nn101081t

Salvador, A.F., Martins, G., Melle-Franco, M., Serpa, R., Stams, A.J.M., Cavaleiro, A.J., Pereira, M.A., Alves, M.M., 2017. Carbon nanotubes accelerate methane production in pure cultures of methanogens and in a syntrophic coculture. Environ. Microbiol. 19, 2727–2739. https://doi.org/10.1111/1462-2920.13774

Şentürk, E., Ince, M., Engin, G.O., 2010. Kinetic evaluation and performance of a mesophilic anaerobic contact reactor treating medium-strength food-processing wastewater. Bioresour. Technol. 101, 3970–3977. https://doi.org/10.1016/j.biortech.2010.01.034

Shen, L., Jin, Z., Wang, D., Wang, Y., Lu, Y., 2018. Enhance wastewater biological treatment through the bacteria induced graphene oxide hydrogel. Chemosphere 190, 201–210. https://doi.org/10.1016/j.chemosphere.2017.09.105

Socrates, G., 2004. Infrared and Raman Characteristic Group Frequencies: Tables and Charts, 3rd

ed. John Wiley and Sons.

Tian, T., Qiao, S., Li, X., Zhang, M., Zhou, J., 2017. Nano-graphene induced positive effects on methanogenesis in anaerobic digestion. Bioresour. Technol. 224, 41–47. https://doi.org/10.1016/j.biortech.2016.10.058

Toral-Sánchez, E., Rangel-Mendez, J.R., Ascacio Valdés, J.A., Aguilar, C.N., Cervantes, F.J., 2017. Tailoring partially reduced graphene oxide as redox mediator for enhanced biotransformation of iopromide under methanogenic and sulfate-reducing conditions. Bioresour. Technol. 223, 269–276. https://doi.org/10.1016/j.biortech.2016.10.062

Trujillo-Reyes, J., Peralta-Videa, J.R., Gardea-Torresdey, J.L., 2014. Supported and unsupported nanomaterials for water and soil remediation: Are they a useful solution for worldwide pollution? J. Hazard. Mater. 280, 487–503. https://doi.org/10.1016/j.jhazmat.2014.08.029

Valenzuela, E.I., Prieto-Davó, A., López-Lozano, N.E., Hernández-Eligio, A., Vega-Alvarado, L., Juárez, K., García-González, A.S., López, M.G., Cervantes, F.J., 2017. Anaerobic Methane Oxidation Driven by Microbial Reduction of Natural Organic Matter in a Tropical Wetland. Appl. Environ. Microbiol. 83, AEM.00645-17. https://doi.org/10.1128/AEM.00645-17

Vance, M.E., Kuiken, T., Vejerano, E.P., McGinnis, S.P., Hochella, M.F., Hull, D.R., 2015. Nanotechnology in the real world: Redeveloping the nanomaterial consumer products inventory. Beilstein J. Nanotechnol. 6, 1769–1780. https://doi.org/10.3762/bjnano.6.181

Vanier, N.L., El Halal, S.L.M., Dias, A.R.G., da Rosa Zavareze, E., 2017. Molecular structure, functionality and applications of oxidized starches: A review. Food Chem. 221, 1546–1559. https://doi.org/10.1016/j.foodchem.2016.10.138

Wang, G., Qian, F., Saltikov, C.W., Jiao, Y., Li, Y., 2011. Microbial reduction of graphene oxide by Shewanella. Nano Res. 4, 563–570. https://doi.org/10.1007/s12274-011-0112-2

Wang, H., Yuan, X., Wu, Y., Huang, H., Peng, X., Zeng, G., Zhong, H., Liang, J., Ren, M.M., 2013. Graphene-based materials: Fabrication, characterization and application for the decontamination of wastewater and wastegas and hydrogen storage/generation. Adv. Colloid

443 Interface Sci. 195–196, 19–40. https://doi.org/10.1016/j.cis.2013.03.009
444 Wang, J., Wang, D., Liu, G., Jin, R., Lu, H., 2014. Enhanced nitrobenzene biotransformation by
445 graphene-anaerobic sludge composite. J. Chem. Technol. Biotechnol. 89, 750–755.
446 https://doi.org/10.1002/jctb.4182
447 Xu, H., Xie, L., Wu, D., Hakkarainen, M., 2016. Immobilized Graphene Oxide Nanosheets as Thin
448 but Strong Nanointerfaces in Biocomposites. ACS Sustain. Chem. Eng. 4, 2211–2222.
449 https://doi.org/10.1021/acssuschemeng.5b01703
450 Xu, S., He, C., Luo, L., Lü, F., He, P., Cui, L., 2015. Comparing activated carbon of different
451 particle sizes on enhancing methane generation in upflow anaerobic digester. Bioresour.
452 Technol. 196, 606–612. https://doi.org/10.1016/j.biortech.2015.08.018
453 Yang, Y., Yu, Z., Nosaka, T., Doudrick, K., Hristovski, K., Herckes, P., Westerhoff, P., 2015.
454 Interaction of carbonaceous nanomaterials with wastewater biomass. Front. Environ. Sci. Eng.
455 9, 823–831. https://doi.org/10.1007/s11783-015-0787-9
456 Zhang, H., Yu, X., Guo, D., Qu, B., Zhang, M., Li, Q., Wang, T., 2013. Synthesis of Bacteria
457 Promoted Reduced Graphene Oxide-Nickel Sulfide Networks for Advanced Supercapacitors.
458 ACS Appl. Mater. Interfaces 5, 7335–7340. https://doi.org/10.1021/am401680m
459 Zhao, J., Wang, Z., White, J.C., Xing, B., 2014. Graphene in the aquatic environment: Adsorption,
460 dispersion, toxicity and transformation. Environ. Sci. Technol. 48, 9995–10009.
461 https://doi.org/10.1021/es5022679
462 Zou, X., Zhang, L., Wang, Z., Luo, Y., 2016. Mechanisms of the Antimicrobial Activities of
463 Graphene Materials. J. Am. Chem. Soc. 138, 2064–2077. https://doi.org/10.1021/jacs.5b11411
464

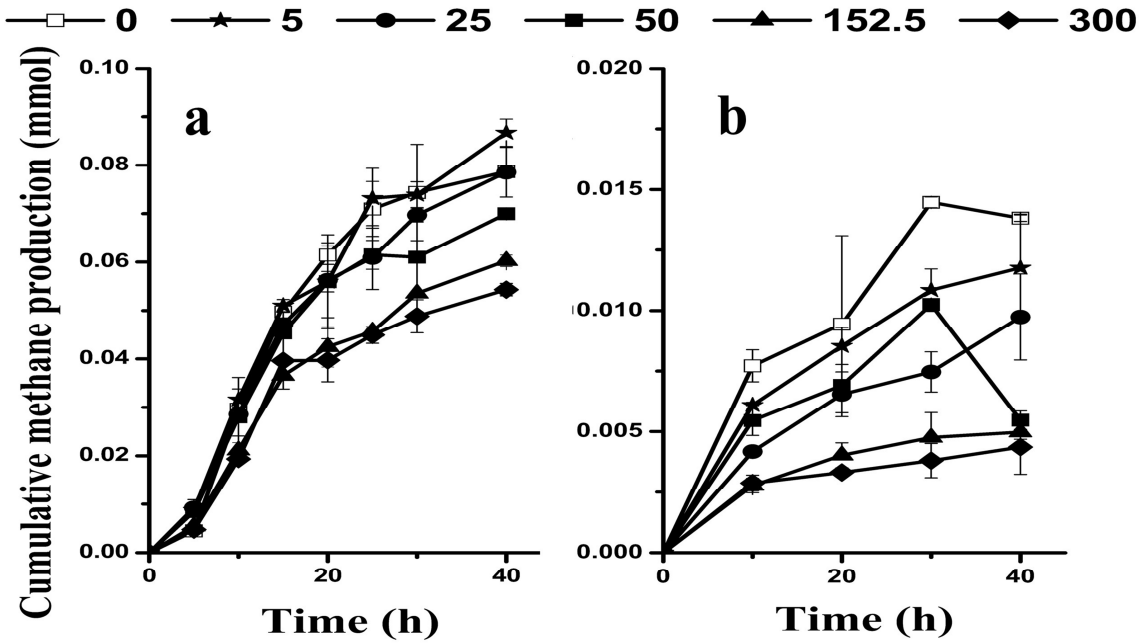

Figure 1. Cumulative methane production by anaerobic sludge supplied with 100 mg COD L^{-1} as glucose (a) and starch (b) as substrates at different GO concentrations (numbers displayed in the series represent GO concentrations in mg L^{-1}).

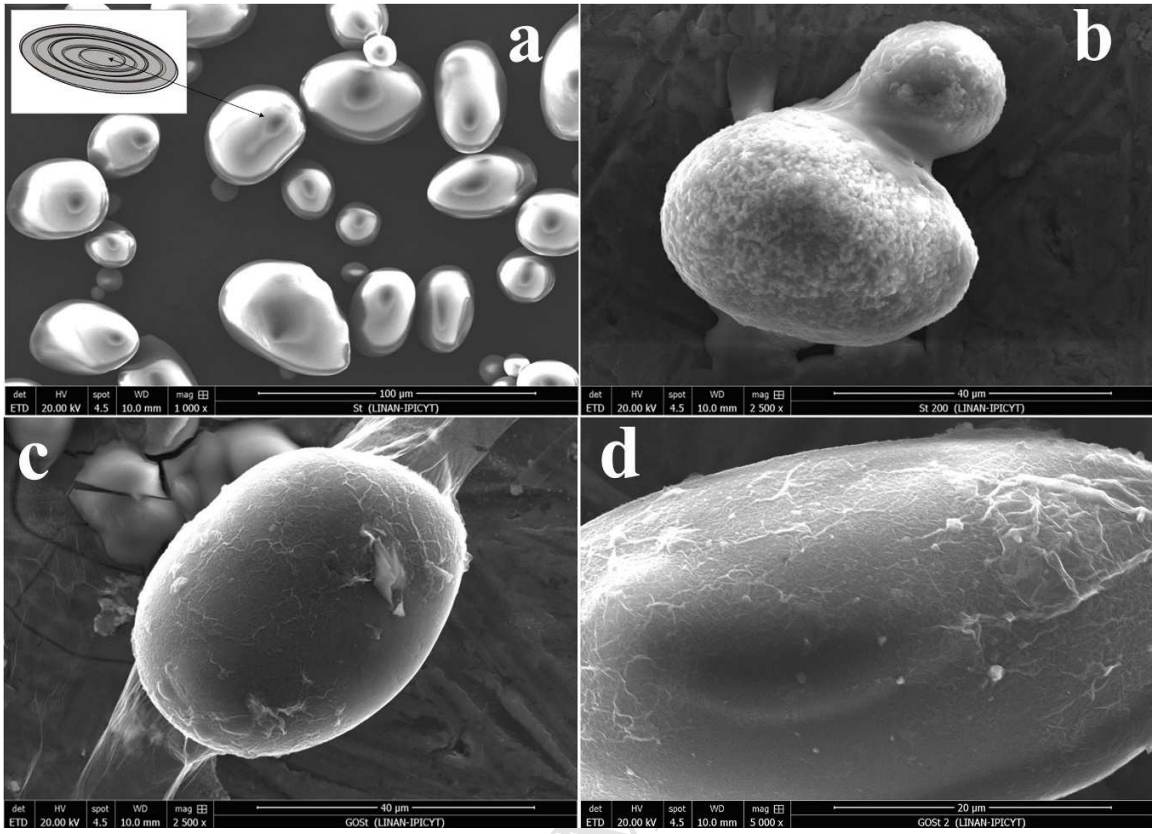

Figure 2. SEM images of starch granules in dry powder form (a) and the schematic growth rings around the hilum identified by the arrow (a inset); granules dispersed in water and dried before observation (b); and starch granules covered with GO sheets (c, d).

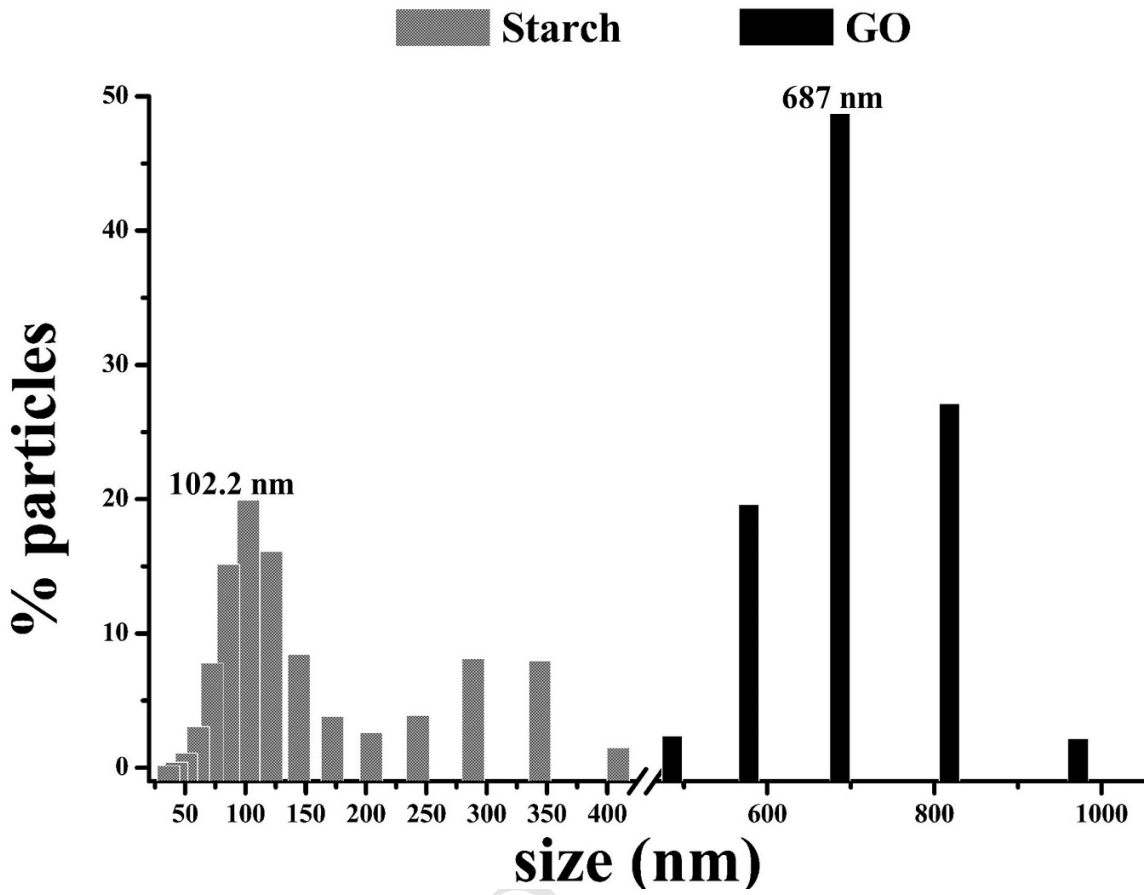

Figure 3. Size distribution obtained by dynamic light scattering of starch (gray) and GO (black) at pH 7 using deionized water as dispersant.

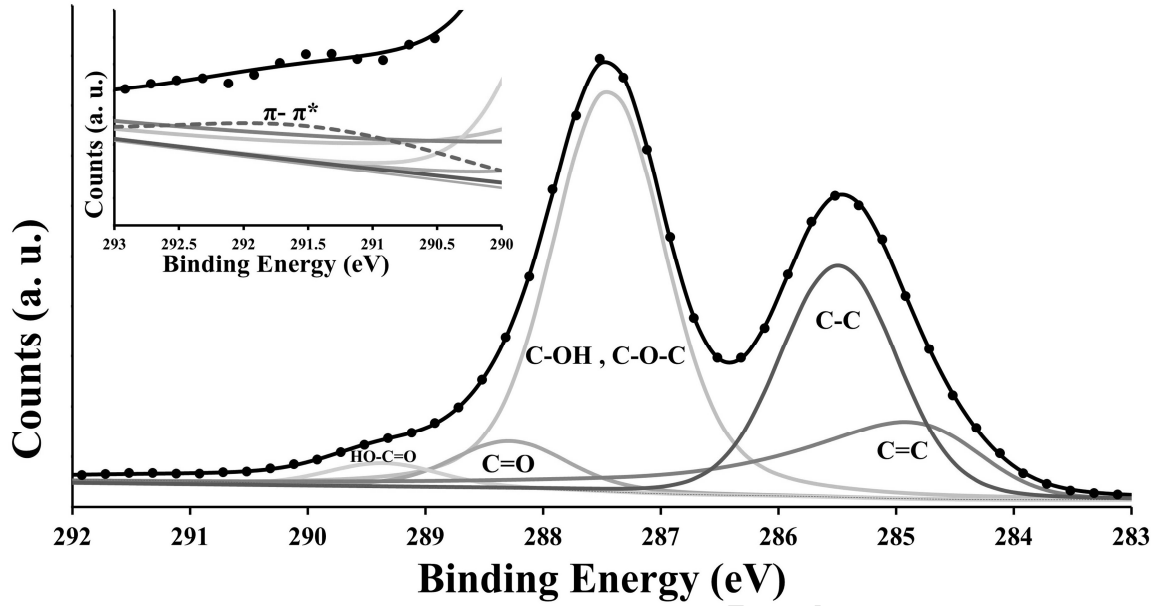

Figure 4. High-resolution C1s X-ray photoelectron spectrum of GO. Dots represent experimental data; solid lines are fitted peaks that identify the different bond types of carbon, and dashed line shows π-π* transitions in aromatic rings (inset).

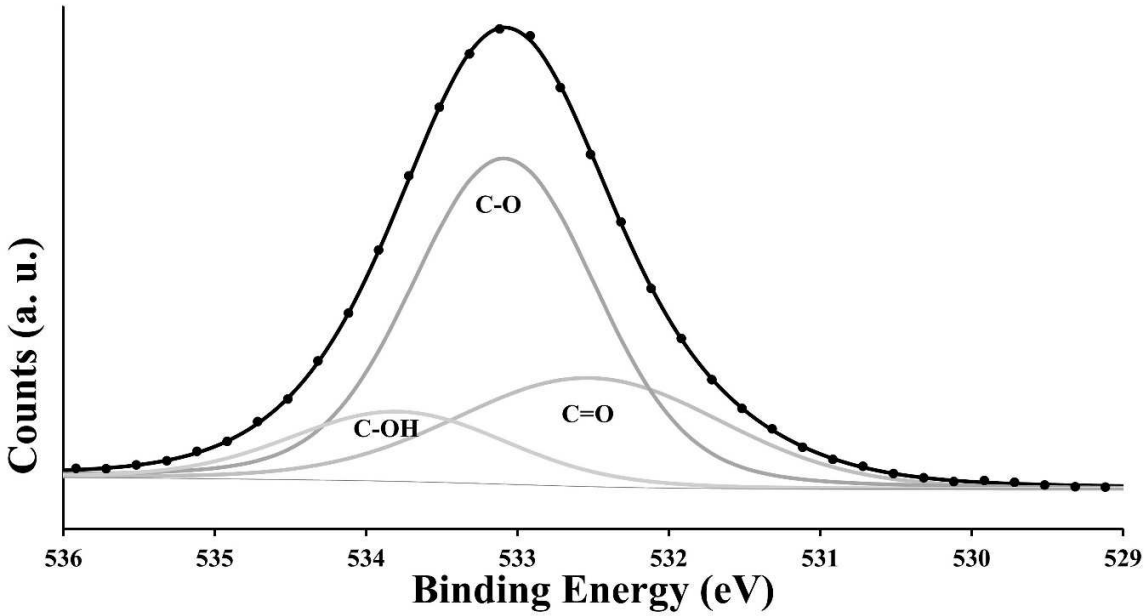

Figure 5. High-resolution O1s X-ray photoelectron spectrum of GO. Grey scale solid lines represent deconvoluted peaks, while dots are experimental data.

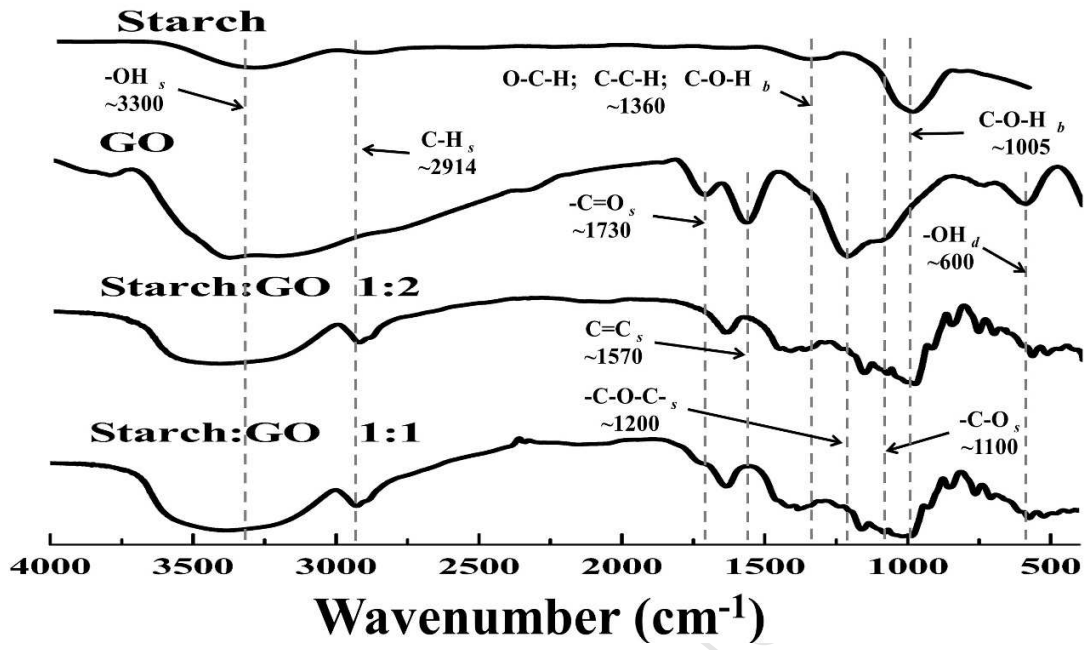

Figure 6. FT-IR spectra of starch, graphene oxide (GO) and starch-GO mixtures with 1:2 and 1:1 ratio, respectively.

Highlights:

- GO wrapped starch granules and prevented their hydrolysis
- Starch granules wrapping with GO sheets was induced by electrostatic attractions
- Methane yield decreased 23.3-fold due to the starch wrapping by GO
- Low GO concentrations showed positive effects on methanogenesis with glucose